ble temperature-dependent effects. The hyperfine A constant shows no such dependence and the scatter is less than the uncertainty on the mean. We therefore use the uncertainty on the weighted mean of the data taken at different temperatures to arrive at an uncertainty of 1 kHz for the hyperfine A constant. For the hyperfine B constant we find an 11 kHz uncertainty (from the scatter of the data).

A theoretical analysis of the frequency dependence on misalignment similar to that described for the $8S_{1/2}$ state analysis yielded a 48 kHz uncertainty for the center-of-gravity frequency and uncertainties of 12 kHz for the hyperfine A constant and 143 kHz for the B constant. In addition, the effects of misalignment were investigated experimentally. Spectra of the six peaks labeled g, h, i, j, k, and l in Fig. 10 were taken at three different beam alignments. The degree of misalignment was characterized by the peak amplitude. Misalignment of the beams so that the peak amplitudes decreased by more than a factor of two resulted in no detectable change in the center-of-gravity, A constant, or B constant.

The uncertainties to the center-of-gravity frequency and the hyperfine A constant are summarized in Table I.

With the uncertainties from Table I we find

$$\begin{aligned} \nu_{6S_{1/2}:7D_{3/2}} &= 780\,894\,762.250(77)\,\text{MHz} \\ A_{7D_{3/2}} &= 7.386(15)\,\text{MHz} \\ B_{7D_{3/2}} &= -0.18(16)\,\text{MHz}. \end{aligned}$$

These numbers are in good agreement with previous measurements, shown in Table II and lead to a significant improvement in the knowledge of the center-of-gravity frequency.

E. Results for the $7D_{5/2}$ state

Figure 12 shows the experimental fluorescence spectra for excitation of the $7D_{3/2}$ and $7D_{5/2}$ states through the $6P_{3/2}$ state along with the calculated spectra for excitation to the $7D_{3/2}$ and $7D_{5/2}$ states. The spectrum was collected using a 850 nm filter with a 10 nm passband for F1 and a 700 nm filter with a 25 nm passband for F2. The close energy spacing of the $7D_{3/2}$ and $7D_{5/2}$ states did not allow for a selection of only one of the states when excited through the $6P_{3/2}$ state. However, because we were able to determine the $7D_{3/2}$ state energy and hyperfine splitting as described in Section IV D, we were able to fix the frequency of the $7D_{3/2}$ state from these measurements and use the spectrum shown in Fig. 12 to extract information about the $7D_{5/2}$ state. In addition, angular momentum considerations result in much stronger transition probabilities for the $6P_{3/2} \rightarrow 7D_{5/2}$ transition compared to the $6P_{3/2} \rightarrow 7D_{3/2}$ transition. To remove the effect of the overlap, we calculated the $7D_{3/2}$ spectrum through the $6P_{3/2}$ state using the values determined by the $6S_{1/2} \rightarrow 6P_{1/2} \rightarrow 7D_{3/2}$ excitation. Figure 13 shows the contribution of the transitions to the $7D_{3/2}$ to

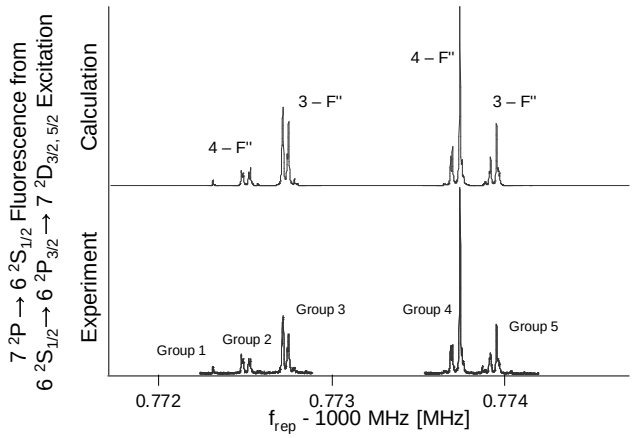

FIG. 12: The calculated spectrum (upper trace) of the 7P → 6S fluorescence when the Cs atoms are excited to the $7D_{3/2,\,5/2}$ state. The experimental signal (lower trace) shows the 7P → 6S fluorescence when the Cs atoms are excited to the both the $7D_{3/2,\,5/2}$ states through the $6P_{3/2}$ state. In the experimental spectrum data are shown for only those regions where there was a signal.

the fluorescence spectrum. We superposed that calculated spectrum on the experimental spectrum and adjusted the peak intensities to match the isolated $7D_{3/2}$ peaks. In this way we accounted for and removed the $7D_{3/2}$ parameters. To quantify the influence of the $7D_{3/2}$ state and estimate the uncertainty resulting from the overlapped spectra, we fit the spectra with and without subtracting the spectrum from the $7D_{3/2}$ state. We found a maximum deviation of 10 kHz in the center-of-gravity frequency of the $7D_{5/2}$ state, 1 kHz in the hyperfine A constant, and 30 kHz in the hyperfine B constant which we take to be the uncertainties due to this overlap. The contributions from the two transitions are separated in Fig. 13.

For a given ground state hyperfine component F, there are nine distinct transitions due to the manifold of intermediate states and upper states. The five groups of peaks labeled in Fig. 12 were used to extract values for the center-of-gravity and hyperfine A and B constants. In group one, only three peaks were of sufficient amplitude to be fit. All nine peaks were fit in groups three and five. Seven peaks were used in group two and six peaks in group four. From the fit to these 34 peaks we determined the center-of-gravity frequency to be 781 522 153.682(25) MHz and the hyperfine A and B constants were $-1.717(4)$ MHz and $-0.182(86)$ MHz, respectively. To improve the precision of the fits, we use scans with increasing frequency and decreasing frequency simultaneously. The minimum χ^2 was 90 for 34 peaks prior to normalization.

The systematics were studied in the same way as with the previous states. We focused on group four of Fig. 13 due to its size and also the fact that there is very little contribution from the $7D_{3/2}$ state for this group. The optical intensity was varied for both stages of the